

Influence of subretinal fluid in advanced stage retinopathy of prematurity on proangiogenic response and cell proliferation

Jie Ma,¹ Manisha Mehta,² Godfrey Lam,¹ Desireé Cyr,¹ Tat Fong Ng,¹ Tatsuo Hirose,¹ Khaled A. Tawansy,³ Andrew W. Taylor,⁴ Kameran Lashkari¹

¹Schepens Eye Research Institute, Mass. Eye and Ear, Department of Ophthalmology, Harvard Medical School, Boston, MA;

²Department of Pathology, Boston University School of Medicine, Boston, MA; ³Children's Retina Institute, Los Angeles, CA;

⁴Department of Ophthalmology, Boston University School of Medicine, Boston MA

Purpose: The clinical phenotype of advanced stage retinopathy of prematurity (ROP, stages 4 and 5) cannot be replicated in an animal model. To dissect the molecular events that can lead up to advanced ROP, we examined subretinal fluid (SRF) and surgically dissected retrolental membranes from patients with advanced ROP to evaluate its influences on cell proliferation, angiogenic properties, and macrophage polarity.

Methods: We compared our findings to SRF collected from patients with uncomplicated rhegmatogenous retinal detachment (RD) without proliferative vitreoretinopathy and surgically dissected epiretinal membrane from eyes with macular pucker. All subretinal fluid samples were equalized for protein. The angiogenic potential of SRF from ROP eyes was measured using a combination of capillary cord formation in a fibrin clot assay, and its proliferative effect was tested with a DNA synthesis of human retinal microvascular endothelial cells. Findings were compared with SRF collected from participants with uncomplicated rhegmatogenous RD without proliferative vitreoretinopathy. The ability of SRF to induce nitric oxide production was measured in vitro using murine J774A.1 macrophages. Cytokine profiles of SRF from ROP and RD eyes were measured using a multienzyme-linked immunosorbent assay (ELISA). Fluorescent immunohistochemistry of retrolental membranes from ROP was performed to detect the presence of leukocytes and the composition of tissue macrophages using markers for M1 and M2 differentiation.

Results: The cytokine composition in SRF revealed that in ROP, not only were several proangiogenic factors were preferentially elevated but also the profile of proinflammatory factors was also increased compared to the RD eyes. SRF from ROP eyes supported cell proliferation and endothelial cord formation while SRF from RD eyes had inhibitory effects. SRF from eyes with ROP but not RD robustly induced nitric oxide production in macrophages. Furthermore, fluorescent immunostaining revealed a preponderance of M1 over M2 macrophages in retrolental fibrous membranes from ROP eyes. The cytokine profile and biologic properties of SRF in ROP promote a proangiogenic environment, which supports the maintenance and proliferation of fibrous membranes associated with advanced stages of ROP. In contrast, SRF from RD eyes exhibits a suppressive environment for endothelial cell proliferation and angiogenesis.

Conclusions: Our investigation demonstrates that the microenvironment in advanced ROP eyes is proangiogenic and proinflammatory. These findings suggest that management of advanced ROP should not be limited to the surgical removal of the fibrovascular membranes and antiangiogenic therapy but also directed to anti-inflammatory therapy and to promote M2 activation over M1 activity.

Retinopathy of prematurity (ROP) is one of the leading causes of neonatal blindness in developed countries [1-4]. From the 16th week of gestation to birth, retinal blood vessels grow from the optic nerve to reach the peripheral retina [1]. However, premature birth and oxygen supplementation can arrest vascularization and form a defined border between the avascular and vascular retina [5]. Once the retina returns to ambient oxygen, vascular proliferation at this junction can induce the development of fibrovascular tissue (corresponding to clinical stage 3 ROP) [5]. In advanced stage

ROP, intense neovascularization encompasses the peripheral retinal surface forming fibrous tissues that contract and induce partial or total retinal detachment (stages 4 and 5, respectively) [1]. Accordingly, stage 5 ROP is characterized by a sequence of events including formation of a dense fibrovascular membrane that encompasses the entire inner retinal surface, contracts, producing funnel-shaped retinal detachment, and accumulation of proteinaceous fluid in the subretinal space [1]. Thus, blindness in ROP is the result of progressive, unrelenting neovascularization and ensuing retinal detachment and photoreceptor degeneration.

Neovascularization is regulated by a complex interplay between cytokines and immune cells, and usually includes a late stage inflammatory response. Angiogenesis is stimulated by the release of factors such as vascular endothelial

Correspondence to: Kameran Lashkari, Schepens Eye Research Institute, Massachusetts Eye and Ear, Harvard Medical School, 20 Staniford Street, Boston 02114, MA, Phone: (617) 912-7464; FAX: (617) 912-0101; email: kameran_lashkari@meei.harvard.edu

growth factor A (VEGF-A), platelet-derived growth factor (PDGF), and tumor necrosis factor α (TNF- α) among others [6]. VEGF-A, in particular, is elevated in early stages of ROP [7]. Ischemic sites also release chemotactic factors to recruit macrophages to the area, which further secrete VEGF-A to promote neovascularization [8,9]. Macrophages exhibit significant plasticity that allows them to change their phenotype depending on their environment. M1 macrophages are generally considered classically activated by interferon- γ (IFN- γ) or lipopolysaccharide (LPS) and exhibit proinflammatory properties. Alternatively activated M2 macrophages exhibit anti-inflammatory properties and are induced by interleukin-4 (IL-4) and IL-13 [10]. In the eye, macrophages are implicated in fibrovascular pathologies, including proliferative diabetic retinopathy, choroidal neovascularization [11], and experimental oxygen-induced retinopathy, a model for early stage ROP [12]. It has been observed that inactivation of the monocyte lineage leads to suppression of pathologic angiogenesis in animals [13]. M1 polarized macrophages are associated with certain inflammatory ocular diseases such as age-related macular degeneration, while M2 macrophages have been described in a murine model of ischemic retinopathy, in which they participate in tissue remodeling [14].

Although capillary obliteration and endothelial proliferation seen in early stages of ROP have been successfully replicated in animal models of oxygen-induced retinopathy [13], the advanced stage of the disease has yet to be induced in an animal model. In humans, advanced ROP is managed through dissecting fibrous membranes and releasing subretinal fluid (SRF) in an effort to reattach the detached retina. Unfortunately, photoreceptor loss, retinal degeneration, and visual disability persist. Surgical specimens can be obtained from normally discarded tissue, including retrolental membranes (which cover the inner surface of the detached retina) and SRF filling the space between the detached retina and the RPE. These samples can be analyzed to understand the condition of the retinal microenvironment associated with advanced stages of ROP. In this study, we analyzed the cytokine profile of SRF and the proangiogenic and proliferative potential of SRF, and compared our findings with those for SRF collected from retinal detachment without proliferative vitreoretinopathy.

METHODS

Specimen collection: Human SRF samples ($n = 12$) and retrolental membranes ($n = 12$) were obtained from 14 patients (ages, 4–8 months) who were undergoing open-sky vitrectomy for stage 5 ROP. Retrolental membranes in stage 5 ROP were bluntly dissected from the underlying detached retina.

SRF was tapped externally into a tuberculin syringe only when clinically indicated. Effort was made to ensure that SRF was not contaminated with blood. Patients with other known concurrent ocular conditions such as glaucoma, congenital anomalies, or inflammatory diseases were excluded. SRF samples were collected from patients who had developed acute retinal detachment (RD) of less than 48 h onset as the control samples. SRF samples were centrifuged at 16,128 *ref* at 4 °C for 20 min, and supernatants were aliquoted for further experiments.

Ethics statement: This study was approved by the Institution Review Boards (IRBs) of Massachusetts Eye and Ear and Schepens Eye Research Institute. The study protocol adhered to the Declaration of Helsinki for research involving human patients. The participants provided written consent and approved the consent procedure for our studies. The study was discussed in detail with the parents or legal guardians. After discussing any questions and concerns, a detailed IRB-approved consent form was presented to them, and written permission was obtained. These specimens were collected from patients who signed the appropriate consent forms and had agreed to participate in the study.

Bio-Plex cytokine array: The Bio-Plex human cytokine 22-Plex panel (Bio-Rad Laboratories, Hercules, CA) was used to measure cytokine composition and concentration in the SRF of patients with ROP and RD. Antibodies used in this cytokine array included Eotaxin, granulocyte colony-stimulating factor (G-CSF), granulocyte-macrophage (GM)-CSF, IFN- γ , IL-1ra, IL-4, IL-5, IL-6, IL-7, IL-8, IL-9, IL-10, IL-12p70, IL-13, IL-15, interferon gamma-induced protein 10 (IP-10), macrophage inflammatory protein 1 α (MIP-1 α), MIP-1 β , regulated and normal T cell expressed and secreted (CCL5) (RANTES), PDGF-BB, TNF- α , and VEGF-A. The procedure has been reported in previous studies [15,16]. Briefly, a 96-well filter plate was wetted with 100 μ l assay buffer solution and vacuum filtered. Anticytokine bead solution (50 μ l) was added to each well, followed by vacuum filtration and two successive buffer washes. SRF samples were diluted sixfold with human serum diluent (Bio-Rad Laboratories), and 50 μ l diluted samples was added to each well. Wells were shaken at 37 shakes per s, 0.5 shakes per s, vacuum filtered, and washed with buffer three times. Detection antibody (25 μ l) was added per well, and the shaking and washing procedure was repeated. Streptavidin-PE (50 μ l) was then added to each well, shaken at 0.5 shakes per s, vacuum filtered, and washed with buffer. After a final shaking at 37 shakes per s, the plate was docked for reading by the automated assay machine (Bio-Plex 200 System, Bio-Rad).

Cell proliferation assay: DNA proliferation assay was performed using human retinal microvascular endothelial cells (HRMECs) kindly provided by Dr. Patricia D'Amore (Schepens Eye Research Institute/Mass Eye and Ear, Boston, MA). Cells were plated at a sub-confluent density of 1×10^3 cells/well in a 96-well plate in EBM-2 medium (endothelial cell growth media kits, Lonza) supplemented with growth factors for 24 h (37 °C, 5% CO₂). The medium was then replaced with basal EBM-2 medium without growth factors, and incubation was continued for 1 day (37 °C, 5% CO₂). Cells were then stimulated with basal EBM-2 medium, 10% SRF from RD eyes (diluted in basic EBM-2 medium), 10% SRF from ROP eyes (diluted in basic EBM-2 medium), or VEGF-A (10 ng/ml, 50 ng/ml, and 100 ng/ml), respectively. After 12 h, a colorimetric proliferation assay (CyQUANT NF Cell Proliferation Assay Kit, Invitrogen, Grand Island, NY) was used to estimate the cell proliferation according to the user instruction. A fluorescence microplate reader with excitation at 485 nm and emission detection at 530 nm was used to measure the fluorescence intensity of each sample. The negative control (basal medium) of cell proliferation was normalized to 100% using the actual value of cell proliferation dividing itself. Similarly, the actual values of cell proliferation yielded in other conditions were used to divide the control for the normalization.

Dead/live cell assay: Dead/live cell assay was performed to determine whether SRF from patients with RD induced endothelial cell toxicity. HRMECs were plated in 96-well plates (2,000 cells/well). After adhesion, wells were washed in 1× PBS (10 mM Na₂HPO₄, 2 mM KH₂PO₄, 2.7 mM KCl; 137 mM NaCl, pH 7.4) and incubated for 24 h in the following media: basal EBM-2 medium, full medium (basal medium with all necessary supplements and growth factors, Lonza), 10% of SRF from patients with RD diluted in basal medium, and 1, 10, and 50 µg/ml mitomycin-C (positive controls). Culture medium was slowly removed from each well. Cells were gently washed in 1× PBS one time. Cells were stained with Calcein AM/EthD-1 (Live/Dead cytotoxicity kit, Invitrogen) according to the manufacturer's instructions. Calcein AM (0.5 µl) and EthD-1 (1.5 µl) were diluted in 1× PBS (2.5 ml; 30–50 µl per well). Cells were imaged and counted for green (live) and red (dead) fluorescence. Cell morphology was also examined under an inverted microscope (Olympus, Model IX51, Avon, MA). Data are presented as the average of the dead cell rate [dead cells/(dead cells + live cells) × 100%].

Angiogenesis assay: Three-dimensional fibrin clot was used for the in vitro angiogenesis assay modified from a previous procedure [17]. Fibrinogen (Sigma, St. Louis, MO) was dissolved in 1× PBS to a concentration of 10 mg/ml and

dialyzed overnight in 1× PBS (pH 7.4) using a drop dialysis method over dialysis paper (Filter 47 mm, 0.025 µm, Millipore, Billerica, MA). This resulted in a protein concentration of 4.3–4.7 mg/ml. Fibrinogen was then sterile-filtered to a final concentration of 1.0–1.5 mg/ml in 1× PBS and added to each well of a 24-well plate. Thrombin (0.635 U/ml; Sigma) was then added, mixed, and pipetted (250 µl) into each well. Fibrin clots were formed at room temperature. Human microdermal capillary endothelial cells (HMCECs, Invitrogen/Cascade Biologics, Portland, OR) 5×10^4 cells per well were added to the surface of the fibrin clots and incubated for 1 h (37 °C, 5% CO₂). The medium was removed, and a top layer of 250 µl fibrinogen/thrombin mixture was pipetted over the cells. SRF from the ROP and RD samples was protein equalized to various concentrations (0.1%, 1.0%, 5.0%, and 10.0%) in Dulbecco's Modified Eagle Medium (DMEM; BioWhittaker, Walkersville, MD) and was placed in wells in a masked fashion. DMEM supplemented with VEGF-A (10 ng/ml) and 0.1% FBS were used as positive and negative controls, respectively. Each assay was performed in triplicate. After 72 h, wells were fixed with 4% paraformaldehyde. Five representative fields per well were photographed with an Olympus inverted microscope. Total mean cord lengths (µm/well) were measured using the NIH Image program (ImageJ 1.46).

Nitrite assay for macrophage activation: Murine J774A.1 macrophages, which have been previously studied [18], were plated at a concentration of 1.5×10^5 cells per well in a 96-well culture plate (37 °C, 5% CO₂) and cultured for 2 h in DMEM with supplements (0.1 M HEPES, 0.1% BSA, 1% nonessential amino acid, 1 µg/ml iron-free transferrin, 10 ng/ml linoleic acid, 0.3 ng/ml Na₂Se and 0.2 µg/ml Fe(NO₃)₃, 2 mM L-glutamine, and 2 mM sodium pyruvate and gentamycin). The supernatants were removed, and the macrophage monolayer was washed twice with fresh medium. Macrophages were incubated (37 °C, 5% CO₂) with *E. coli* LPS (Sigma) at a concentration of 1 µg/ml (positive control), medium (negative control), or with 10% of SRF from the ROP and RD samples (diluted in the same medium). After 24 h, the supernatant (75 µl) from individual wells was mixed with deionized water (65 µl), and the mixture solution (10 µl) of N-1-naphthylethylenediamine-HCl (0.1%) and sulfanilamide (1.0%; volume ratio 1:1) in acetic acid (60%, Griess reagent, Molecular Probes, San Jose, CA). The plate was then incubated for 10 min in the dark as described previously [19]. Nitrite concentration in 100 µl of cell culture supernatant using the Griess reagent was then determined for each well by measuring the optical density at 550 nm [20]. All experiments were done in triplicate.

Tissue preparation and immunohistochemistry: After surgical removal, fibrous membranes were collected from 12 patients with stage 5 ROP and prepared for frozen sections. Sections were incubated with primary antibodies, followed by successive 1× PBS washes (30 min in total) and incubation with fluorescent secondary antibodies Cy2 and Cy3 in the dark for 40 min. Slides were photographed with an Olympus digital inverted microscope. For comparison, ERMs obtained from five patients with macular pucker were subjected to staining and cell count. Fluorescent micrographs of five representative regions from each section were used for cell counting. Cells expressing the marker of interest and total cells per-field were tabulated for each section and calculated as a ratio of positive over total cell number. Positive cells were defined as those exhibiting positive staining for the fluorescent marker in their cytoplasm and possessing nuclei identified with 4',6-diamidino-2-phenylindole (DAPI) staining. The following antibodies were used in immunohistochemistry: CD40 and CD260 (LifeSpan BioSciences, Seattle, WA), inducible nitric oxide synthase (iNOS; R&D System, Minneapolis, MN), and arginase I (LifeSpan BioSciences). Secondary antibodies, Cy2 and Cy3, were purchased from Abcam (Cambridge, MA).

Data analysis: The Student *t* test was used to compare differences in the capillary cord formation of HRMECs cultured in RD and ROP SRF. Other statistical analysis in this study was subjected to the Wilcoxon signed-rank test according to the non-normal distribution. To establish linear regressions, natural logarithm transformation (Ln-transformation) was performed to normalize data collected from the dose-dependent formation of capillary cord induced by SRF from ROP and RD eyes [21]. The data are presented as mean ± standard error of the mean (SEM). All specific analyses and regressions were performed in Sigma Plot 11.0 (San Jose, CA). The level of significance *p* value was set at <0.05.

RESULTS

Angiogenic and inflammatory cytokines in subretinal fluid: Differences in the cytokine expression profiles of SRF from ROP and RD eyes were measured using a multiplex (Bio-Plex) immunoassay. Of the 22 inflammatory cytokines evaluated (Table 1), three had significantly higher levels in the RD samples compared to the ROP samples (G-CSF, IL-6, and IFN- γ , all *p*<0.05). From the same set of cytokines, there were significantly higher amounts of the proangiogenic and proliferative cytokines, VEGF-A and PDGF-BB, and the chemotactic cytokines, MIP-1 α , MIP-1 β , and RANTES (all *p*<0.05) in the SRF from the ROP eyes than in the SRF from the RD eyes. In addition, there was significantly more IL-1ra

in the SRF from the ROP eyes (both *p*<0.05). There were no significant differences in the cytokine concentrations in the SRF for eotaxin, GM-CSF, IL-4, IL-5, IL-7, IL-8, IL-9, IL-10, IL-12p70, IL-13, IL-15, IP-10, and TNF- α (Table 1). These results show that there are differences in the cytokine profiles of SRF from RD and ROP eyes. These differences are related to the expression of more potentially proangiogenic, chemotactic, and proliferative cytokines in the SRF of ROP eyes.

Proliferative effects of subretinal fluid: To further study the biologic effects of proliferative cytokines present in the SRF of ROP eyes, the ability of SRF to induce proliferation in HRMECs was measured. The SRF from ROP eyes significantly promoted proliferation; in contrast, SRF from RD eyes significantly suppressed proliferation. Compared to the medium as the negative control, SRF from ROP eyes induced about an 80% increase in DNA proliferation of HRMECs, respectively. Conversely, SRF from RD eyes inhibited HRMEC proliferation by 50% (Figure 1A). In addition, different concentrations of VEGF-A stimulated HRMECs at least as much as SRF from ROP eyes (156%, 209%, and 145%, respectively; Figure 1A). Statistical significance was measured between every two culture conditions for cell proliferation, and all *p* values are listed in Figure 1B. Our data show that SRF from ROP eyes promoted endothelial cell proliferation, while SRF from RD eyes inhibited this response.

Using the dead/live cell assay, we observed that the mean dead cell rate for HRMECs grown in 10% of RD SRF was low (11.9±0.9%) and similar to that for HRMECs grown in full medium (9.2±4.0%; *p*>0.05). The dead cell rate in basal medium was 19.0±3.7%. In addition, there were no observable differences between the morphology of HRMECs grown in 10% of RD SRF versus those grown in full medium (Figure 1C). In contrast, the mean dead cell rate for cultured HRMECs in various concentrations of mitomycin-C was much higher (21.8±3.1% at 1 μ g/ml, 29.9±6.1% at 10 μ g/ml, and 34.0±2.0% at 50 μ g/ml) than that in RD SRF (all *p*<0.05, Figure 1C). These data confirm that SRF from RD eyes inhibit endothelial cell proliferation without inducing detectable toxic effects on cell survival and morphology in vitro.

Effects of subretinal fluid on capillary cord formation: To evaluate the angiogenic properties of SRF, a three-dimensional fibrin clot model was used. Capillary cord was formed in all culture conditions, and the cord length from medium alone was longer than that from cultured in the mixture medium with SRF from patients with RD (Figure 2A). SRF from ROP eyes at concentrations of 5.0% (11,779±33 μ m) and 10.0% (10,570±33 μ m) significantly enhanced cord length formation compared to the negative control (0.1%

TABLE 1. THE CONCENTRATION (PG/ML) OF CYTOKINES IN SRF FROM ROP AND RD EYES USING BIO-PLEX CYTOKINE ARRAY.

Cytokines	ROP (n=10, min – max)	RD (n=10, min – max)	P
Eotaxin	6.5±0.2 (6.36 – 6.72)	10.7±7.0 (2.70 – 21.78)	≥0.05
G-CSF	76.4±41.7 (34.80 – 117.90)	2421.8±801.9 (366.48 – 2421.78)	<0.001
GM-CSF	26.5±8.1 (18.36 – 34.68)	24.9±4.3 (19.56 – 31.50)	≥0.05
IFN-γ	12.3±1.2 (11.10 – 13.44)	34.0±16.8 (14.88 – 60.54)	<0.05
IL1-ra	11,330.2±5570.0 (5758.38 – 16,902.00)	88.8±32.5 (37.92 – 126.42)	<0.001
IL-4	0.2±0.2 (0.00 – 0.36)	0.7±0.4 (0.18 – 1.38)	≥0.05
IL-5	142.1±132.7 (9.42 – 274.80)	10.1±12.4 (0.00 – 30.30)	≥0.05
IL-6	209.2±52.3 (156.78 – 261.60)	5274.8±2005.4 (2082.00 – 7503.48)	<0.001
IL-7	3.8±1.3 (2.52 – 5.10)	11.6±2.3 (9.48 – 15.48)	≥0.05
IL-8	845.8±776.4 (69.48 – 1622.04)	115.1±21.9 (95.94 – 150.30)	≥0.05
IL-9	24.1±8.4 (15.72 – 32.52)	18.8±5.5 (15.18 – 27.78)	≥0.05
IL-10	11.9±7.8 (4.08 – 19.74)	3.7±1.9 (0.66 – 5.70)	≥0.05
IL-12p70	3.4±1.3 (2.10 – 4.62)	1.8±0.7 (0.66 – 2.58)	≥0.05
IL-13	2.4±0.7 (1.68 – 3.12)	0.9±0.6 (0.06 – 1.62)	≥0.05
IL-15	6.1±5.5 (0.60 – 11.64)	19.6±8.0 (12.90 – 32.64)	≥0.05
IP-10	16,431.9±4567.9 (11,860.74 – 21,000.00)	15,788.5±3248.4 (10,564.86 – 19,198.02)	≥0.05
MIP-1α	13.6±9.3 (4.38 – 22.86)	1.5±0.9 (0.00 – 2.28)	<0.05
MIP-1β	376.1±266.6 (109.44 – 642.78)	63.4±21.3 (33.36 – 93.48)	<0.001
RANTES	950.7±21.2 (929.46 – 971.94)	0.5±0.6 (0.00 – 1.38)	<0.05
PDGF-BB	47.0±9.4 (37.62 – 56.46)	12.1±10.9 (0.00 – 29.40)	<0.05
TNF-α	16.0±0.2 (15.72 – 16.20)	18.7±3.4 (14.52 – 23.88)	>0.05
VEGF-A	11,522.6±3160.1 (8362.20 – 14,682.90)	601.4±389.6 (117.30 – 1200.60)	<0.001

of FBS, 5,910±22 μm; both p<0.05). However, the 0.1% (3,780±30 μm) and 1.0% (7,428±18 μm) concentrations did not show any significant enhancement (both p>0.05; Figure 2A). Compared to the positive control (VEGF-A, 10 ng/ml), SRF from ROP eyes at the concentration of 1.0%, 5.0%, and 10.0% had similar enhancement effects on capillary cord formation (Figure 2A). Conversely, SRF from RD eyes inhibited capillary cord formation. At concentrations of 1.0%, 5.0%, and 10.0%, there was a significant decrease in capillary formation compared to the (0.1% of FBS) negative control (all p<0.05, Figure 2A). At lower concentrations, the effects of SRF from RD eyes on cord length were not significantly different from those of the negative control (p>0.05, Figure 2A). Therefore, SRF from ROP eyes induced capillary tube formation in a positive dose-dependent manner. Specifically, the capillary cord formation was positively associated with the concentration of SRF from ROP eyes, but negatively associated with the concentration of SRF of RD eyes (Figure 2B). These in vitro assays demonstrate that SRF from ROP eyes exhibits proangiogenic properties, while SRF from RD eyes are possibly angiostatic. A detailed comparison (p values) of

SRF on capillary cord formation between every two different culture conditions is listed in Table 2.

Production of nitric oxide from macrophages induced by subretinal fluid: To determine whether SRF from ROP eyes activates macrophages and potentially promotes inflammation, the ability of SRF to induce nitric oxide production in macrophages was assessed. The nitrite levels in the condition media relative to the nitric oxide levels generated by the macrophages was significantly higher in the cultures of macrophages treated with SFR from ROP eyes and at the same level of macrophages stimulated with LPS (Figure 3A). In contrast, SRF from RD eyes stimulated no more nitrate than the macrophages at rest (Figure 3A). Statistical significance was measured between every two culture conditions on nitric oxide production, and all p values are listed in Figure 3B. This demonstrates that along with the proangiogenic activity there is proinflammatory support by the SRF of ROP eyes as suggested by their cytokine profile.

Macrophages in retrolental membranes express MI polarity: Results demonstrate that the SRF from ROP eyes potentially promotes angiogenesis and inflammation. This suggests

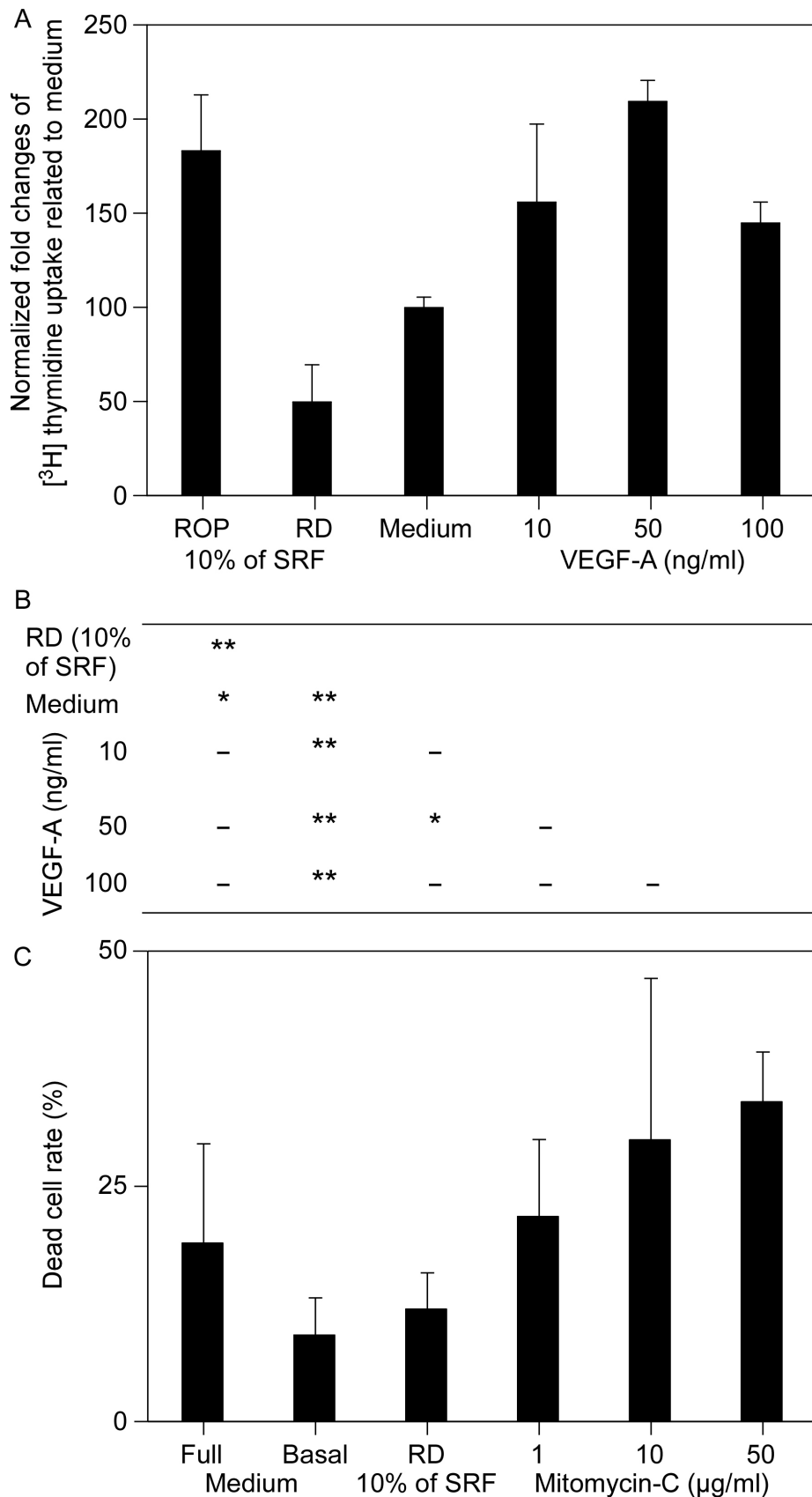


Figure 1. Effects of subretinal fluid from eyes with retinopathy of prematurity and retinal detachment on the proliferation of human retinal microvascular endothelial cells; evaluation of toxic effect of subretinal fluid from patients with retinal detachment on human retinal microvascular endothelial cells. **A:** Data were normalized to the mean values of the human retinal microvascular endothelial cells (HRMECs) grown in medium alone. Subconfluent cultures were incubated with 10% concentrations of subretinal fluid (SRF) from eyes with retinopathy of prematurity (ROP) and retinal detachment (RD). SRF from ROP eyes induced an increase in the proliferation effect while SRF from RD eyes showed a modest inhibitory effect. Vascular endothelial growth factor A (VEGF-A; 10–100 ng/ml) was used as the positive control. **B:** The dead cell rates (the dead cell rate=the number of dead cells/the number of (dead cells + live cells) x 100%) of HRMECs cultured in different conditions.

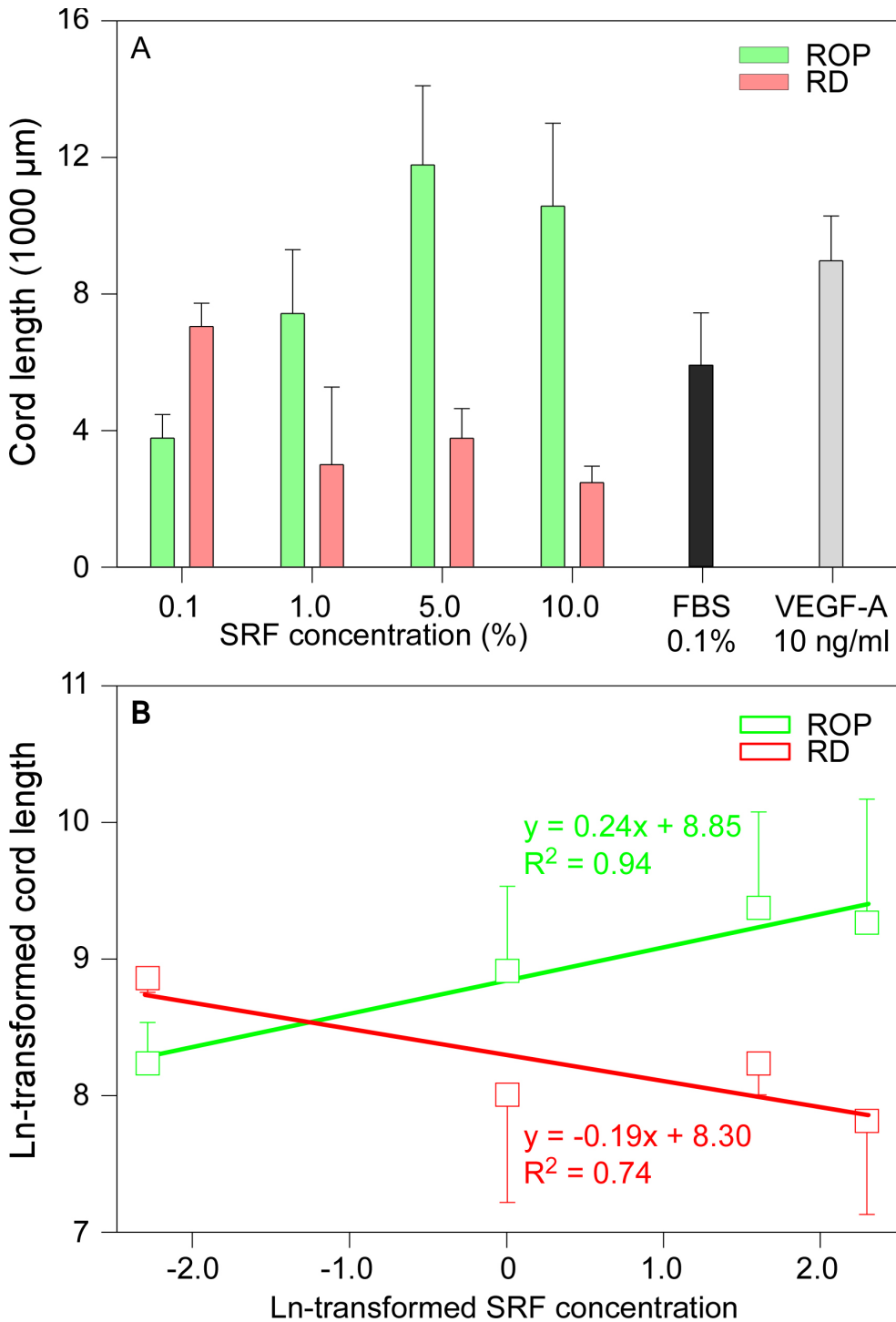


Figure 2. Three-dimensional fibrin clot model of cord formation by human microdermal capillary endothelial cells incubated with subretinal fluid from eyes with retinopathy of prematurity and retinal detachment. The capillary cord was formed in all culture conditions and indicates that the cord length from the medium alone was longer than that from cells cultured in a medium containing SRF from patients with retinal detachment (RD). A: Subretinal fluid (SRF) from eyes with retinopathy of prematurity (ROP) induced cord formation in human microdermal capillary endothelial cells (HMCECs) while SRF from eyes with RD showed shorter length measurements (Student t test, n = 10/group, * p < 0.05, Mean±SEM, please see Table 2 for detailed comparisons). Vascular endothelial growth factor A (VEGF-A; 10 ng/ml) and 0.1% fetal bovine serum (FBS) were used as positive and negative controls, respectively. B: A linear association was found between the cord length and the SRF concentration (ROP, positive; RD, negative). The cord length and the SRF concentration were natural logarithm (Ln)-transformed to establish the linear models.

that monocytes that migrate to the fibrovascular membranes would be polarized to into either M1 macrophages to mediate inflammation or to M2 macrophages that would contribute to the proangiogenic state of the SRF. Immunostaining of these membranes for CD40 and CD206 (representing M1 and M2 polarity, respectively) showed a preponderance of CD40 over

CD206 markers (Figure 4A). Expression of the M1 intracellular enzyme iNOS and the M2 intracellular enzyme arginase 1 was sporadic (Figure 4B–C). Overall, the expression of M1 over M2 markers in retrolental membranes from ROP eyes increased eightfold (88.8±7.0% versus 11.2±7.0%, p<0.001, Figure 4D). This demonstrates that these proangiogenic and

TABLE 2. PAIRWISE MULTIPLE COMPARISON OF SRF ON CAPILLARY CORD FORMATION BETWEEN EVERY TWO CULTURE CONDITIONS (P VALUES).

Culture media	0.1% of FBS	10 ng/ml of VEGF	0.1% of ROP	1.0% of ROP	5.0% of ROP
10 ng/ml of VEGF	0.000				
0.1% of ROP	0.093	0.083			
1.0% of ROP	0.338	0.565	0.034		
5.0% of ROP	0.520	0.903	0.254	0.795	
10.0% of ROP	0.048	0.576	0.010	0.150	0.599
Culture media	0.1% of FBS	10 ng/ml of VEGF	0.1% of RD	1.0% of RD	5.0% of RD
10 ng/ml of VEGF	0.000				
0.1% of RD	0.306	0.441			
1.0% of RD	0.140	0.082	0.042		
5.0% of RD	0.104	0.084	0.007	0.613	
10.0% of RD	0.021	0.044	0.001	0.716	0.087
Culture media		0.1% of ROP	1.0% of ROP	5.0% of ROP	10.0% of ROP
0.1% of RD		0.004	0.757	0.711	0.073
1.0% of RD		0.600	0.060	0.217	0.017
5.0% of RD		0.990	0.037	0.254	0.010
10.0% of RD		0.055	0.011	0.162	0.005

proinflammatory cytokines mediate development of M1 and M2 macrophage polarity in the fibrous membranes of eyes with ROP.

DISCUSSION

We evaluated the cytokine levels in the SRF from young patients with ROP and RD. The measurements indicated that the concentration varied among individuals. ROP is not a common eye disease, and collecting enough SRF from patients with ROP to make a meaningful analysis is difficult. Recent studies showed that among 383 preterm infants screened for ROP, only one had stage 5 disease [22]. Additionally, in most cases, SRF is not routinely drained (and collected) during surgical collection of advanced stage ROP. Therefore, collecting a large sample of SRF is difficult since advanced ROP is an orphan disease and surgical drainage of SRF is not routinely performed. A previous study indicates that the protein concentration of SRF varies with the duration of RD [23]. Thus, it may be easy to observe individual variations in the cytokine concentration in these patients. This leads to the large standard divisions. In addition, the cytokine concentration in SRF covered a wide range in a recent study even though the cytokine levels were calculated from an appropriately large sample population [24].

ROP is a condition in which the hyperoxic environment inhibits programmed (and possibly VEGF-driven) retinal

vasculogenesis [25], and the early stage has been recapitulated in the oxygen-induced model of retinopathy [13]. In this model, the normal vascularization pattern is interrupted, as blood vessels fail in their progress to reach the ora serrata of the retina [26]. When animals are returned to ambient oxygen, the avascular retina releases VEGF-A and other factors to induce vessel growth [25]. This robust fibrovascular response promotes endothelial cell proliferation and migration beyond the inner limiting membrane of the retina and toward the vitreous cavity, forming atypical fibrous tissues, which can exert traction on the retina and cause its detachment [1]. We supposed that SRF from patients with ROP would enhance cell proliferation and vessel formation because one of the typical clinical characteristics of ROP is the development of fibrovascular tissue that can lead to partial or total retinal detachment [1]. This also indicates that SRF from patients with ROP enhances human cellular and fibrous proliferation. The Bio-Plex cytokine array analysis indicates that the concentration of VEGF-A in SRF was relatively high (11,522.6 pg/ml). Previous studies proved that VEGF-A could significantly provoke fibrous proliferation [27-30] in a broad aspect from human to low-level vertebrates. We therefore performed our proliferation assays on HRMECs, representing microvascular and macrovascular cells. In the current study, medium of SRF from patients with ROP had significant effects on proliferation even though the cytokine concentration was relatively low in the culture condition.

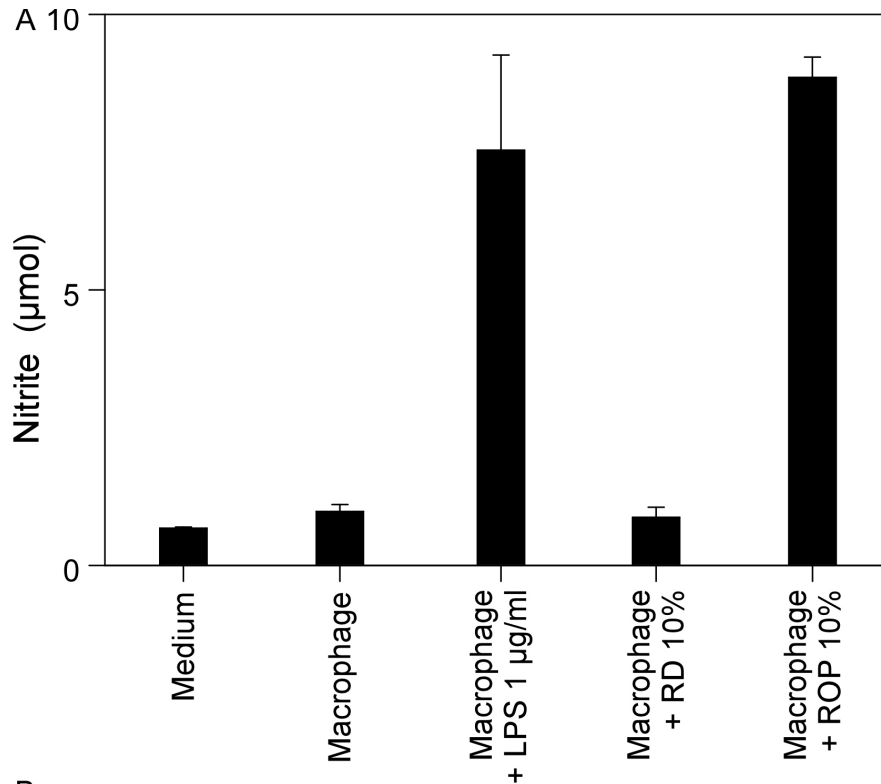


Figure 3. Nitrite production in cultured macrophages incubated with subretinal fluid from eyes with retinopathy of prematurity and retinal detachment. **A:** Subretinal fluid (SRF) from eyes with retinopathy of prematurity (ROP) induced robust production of nitrite at levels similar to lipopolysaccharide (LPS; positive control; Wilcoxon signed-rank test, - $p \geq 0.05$, * $p < 0.05$, ** $p < 0.001$). SRF from eyes with retinal detachment (RD) did not have any measurable effects. **B:** Detailed comparison of nitrite production between every two different conditions, for instance, $p > 0.05$ between macrophage and medium, $p < 0.05$ between macrophage + LPS 1 µg/ml versus medium.

B

Macrophage	-			
Macrophage + LPS 1 µg/ml	*	*		
Macrophage + RD 10%	-	-	*	
Macrophage + ROP 10%	**	**	-	**

Based on this observation, we postulate that the cytokine concentration in SRF from patients with ROP could be high enough to enhance the proliferation and angiogenesis in vivo.

In the early clinical stages of ROP, the fibrovascular tissue generally regresses, and normal retinal vascularization resumes. However, little is known about advanced stage ROP and why eyes with early stage ROP progress to more advanced stages, as this phenomenon cannot be replicated in an animal model. In this study, we extracted SRF and fibrovascular membranes from patients with advanced ROP and analyzed their cytokine profile and distribution of immune cells involved to better define the molecular and cellular participants of advanced ROP. In vitro assays for capillary formation and endothelial proliferation showed that SRF from ROP eyes induced robust support for these cellular processes similar to VEGF-A. Interestingly, SRF from RD

eyes showed inhibitory effects on both processes. This inhibitory effect diminished with dilution suggesting the presence of an inhibitor. In the present study, HMCECs were used to study cord structure formation instead of using HRMECs, which have been used to study the formation of capillary or capillary-like structures in vitro [31-33]. For an additional comparison to HRMECs, we used HMCECs to evaluate the ability of VEGF-A on the formation of capillary-like structures. Continuous neurovascular development in the retina is a typical feature of ROP, and VEGF-A plays an important role in stimulating vasculogenesis and angiogenesis. When we assayed SRF from ROP eyes, we observed that proangiogenic cytokines VEGF-A and PDGF-BB were elevated compared to SRF from RD eyes. In comparison, G-CSF, IFN- γ , and IL-6 associated with acute inflammation, antigen presentation, and subsequent cell-mediated responses had lower concentrations

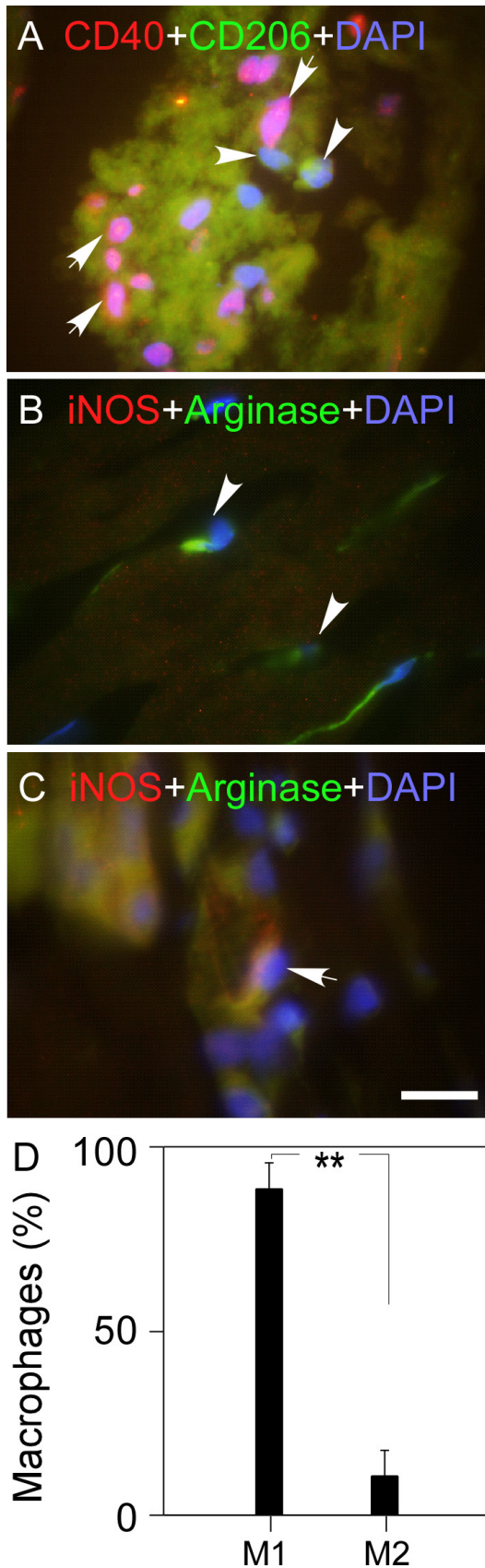


Figure 4. Immunohistochemical localization for macrophages in retrolental membranes from eyes with retinopathy of prematurity. **A**: Expression of CD40 (representing M1 polarity; arrows) and CD206 markers (representing M2 polarity; arrowheads) in tissue macrophages associated with retinopathy of prematurity (ROP) tissue. **B–C**: Antihuman inducible nitric oxide synthase (iNOS) and arginase antibodies were also used to detect M1 and M2 macrophages, respectively. **D**: Distribution of M1 and M2 macrophages in retrolental membranes from eyes with retinopathy of prematurity (ROP); the predominant macrophage is the M1 type, and there is only a limited number of M2 type macrophages (** $p < 0.001$). Scale bar = 20 μm .

in the ROP specimens than in the RD specimens. These findings correlate with the pathophysiology of RD as an acute inflammatory or wound healing process [34].

Our results show that in the membranes of ROP eyes there is a mix of M1 and M2 macrophages with M1 macrophages outnumbering M2 macrophages. Therefore, these membranes harbor proangiogenic M2 macrophages. The lack of significant levels of proinflammatory cytokines suggests that the M1 macrophages are either inactive or are a source of the chemokines that promote cellular infiltration. It is also possible that they arose from an earlier inflammatory response. This would suggest the neovascularization in advanced ROP might well be a result of an inflammatory response that transitions to an unregulated M2 wound repair response. The results clearly demonstrate that retinal microenvironment of advanced ROP is proangiogenic and proinflammatory.

Numerous cytokine studies are available, but there is not much comparable data on cytokine concentration of SRF from young patients with ROP. Compared to the cytokine concentration in SRF of patients with RD in a previous study [24], the levels of proinflammatory cytokines were much higher in our study, including IL-6 (209.2 pg/ml versus 60 pg/ml), INF- γ (12.3 pg/ml versus <0.3 pg/ml), TNF- α (16.0 pg/ml versus 6.2 pg/ml), and IL-15 (6.1 pg/ml versus 0.8 pg/ml). M1 macrophages secrete many cytokines, such as IL-6 and TNF- α . The concentrations of proinflammatory cytokines, which are closely related to M1 macrophages, are relatively high in our study. This might be largely due to the eightfold higher number of M1 macrophages compared to M2 macrophages detected in the retrolental membranes of patients with ROP. In our study, the medium with SRF of patients with ROP had significant effects on proliferation and angiogenesis even though the actual cytokine concentration was relatively low in the culture condition. Therefore, we supposed that the SRF of patients with ROP must be high enough to enhance proliferation and angiogenesis *in vivo*.

In the culture situation, we did not find obviously toxic effects on the antiproliferation of HRMECs. HRMECs grew quite well in the medium with SRF from the patients with RD although the proliferation was significantly slower compared to other culture situations. However, an exaggerated inflammatory response was observed in some patients with RD [24], and an accumulation of lactic acid and dextrose was found in patients with long-duration RD [23]. Phospholipids are also increased in SRF, which reflects increased apoptosis leading to retinal degeneration [23]. (Phosphatidylserine externalization expressed on the outer membrane of apoptotic cells is the “eat me” signal for phagocytes [35]). HRMECs were also

used to estimate the toxic effect of SRF from patients with RD. But no such toxic effects were observed on the survival and morphology of HRMECs *in vitro*.

Our findings implicate macrophages in fibrovascular membranes and their specific products such as proangiogenic cytokines (found in the SRF) to transition from early to advanced stage ROP. Suppression of angiogenic and proliferative cytokines, in particular VEGF-A and PDGF-BB, may prevent disease progression from earlier stages. This is supported by recent evidence that anti-VEGF-A agents such as bevacizumab (Avastin) can control and slow progression of ROP [36]. However, in parallel to anti-VEGF-A therapy, strong consideration should be given to anti-inflammatory therapy to control the deleterious actions of M1 macrophages and possibly recruitment of microglia. For example, down-regulation of MIP-1 α and MIP-1 β can reduce macrophage recruitment and diminish their role in neovascularization and inflammation. Possible combinatorial therapy including antiangiogenic and anti-inflammatory agents could have a strong positive clinical effect in controlling the progression of advanced ROP.

The cytokine profile and biologic properties of SRF from ROP eyes promote a proangiogenic environment that supports the maintenance and proliferation of fibrovascular membranes associated with advanced stages of ROP. In contrast, the properties of SRF from RD eyes exhibit a suppressive environment for endothelial cell proliferation and angiogenesis. Induction of iNOS by SRF from ROP eyes *in vitro* and the observed preponderance of CD40 positive over CD206 positive macrophages in fibrovascular tissues suggest predominance of M1 over M2 polarity and support a potentially strong concurrent proinflammatory environment. These findings suggest that management of advanced ROP should not be limited to antiangiogenic therapy but also target the inflammatory component.

ACKNOWLEDGMENTS

The authors thank Drs. Andrius Kazlauskas and Patricia D’Amore from Schepens Eye Research Institute for kindly providing porcine aortic endothelial cells and human retinal microvascular endothelial cells, respectively, and for their helpful review and comments on the manuscript. This study was supported in part by a grant from the Canary Charitable Foundation, NY, NY and by the Stone Scholar Fund, Schepens Eye Research Institute (to KL).

REFERENCES

1. Peterson RA, Hunter DG, Mukai S. Principles and practice of ophthalmology. Philadelphia: W.B. Saunders Company. 1994; 746 p.
2. Zepeda-Romero LC, Barrera-de-Leon JC, Camacho-Choza C, Gonzalez Bernal C, Camarena-Garcia E, Diaz-Alatorre C, Gutierrez-Padilla JA, Gilbert C. Retinopathy of prematurity as a major cause of severe visual impairment and blindness in children in schools for the blind in Guadalajara city, Mexico. *Br J Ophthalmol* 2011; 95:1502-5. [PMID: 21653214].
3. Chen J, Joyal J-S, Hatton CJ, Juan AM, Pei DT, Hurst CG, Xu D, Stahl A, Hellstrom A, Smith LEH. Propranolol inhibition of β -adrenergic receptor does not suppress pathologic neovascularization in oxygen-induced retinopathy. *Invest Ophthalmol Vis Sci* 2012; 53:2968-77. [PMID: 22491401].
4. Chen J, Smith LH. Retinopathy of prematurity. *Angiogenesis* 2007; 10:133-40. [PMID: 17332988].
5. Lucey JF, Dangman B. A reexamination of the role of oxygen in retrolental fibroplasia. *Pediatrics* 1984; 73:82-96. [PMID: 6419199].
6. Damert A, Machein M, Breier G, Fujita MQ, Hanahan D, Risau W, Plate KH. Up-regulation of vascular endothelial growth factor expression in a rat glioma is conferred by two distinct hypoxia-driven mechanisms. *Cancer Res* 1997; 57:3860-4. [PMID: 9288800].
7. Alon T, Hemo I, Itin A, Pe'er J, Stone J, Keshet E. Vascular endothelial growth factor acts as a survival factor for newly formed retinal vessels and has implications for retinopathy of prematurity. *Nat Med* 1995; 1:1024-8. [PMID: 7489357].
8. Davies MH, Eubanks JP, Powers MR. Microglia and macrophages are increased in response to ischemia-induced retinopathy in the mouse retina. *Mol Vis* 2006; 12:467-77. [PMID: 16710171].
9. Afzal A, Shaw LC, Ljubimov AV, Boulton ME, Segal MS, Grant MB. Retinal and choroidal microangiopathies: therapeutic opportunities. *Microvasc Res* 2007; 74:131-44. [PMID: 17585951].
10. Galdiero MR, Garlanda C, Jaillon S, Marone G, Mantovani A. Tumor associated macrophages and neutrophils in tumor progression. *J Cell Physiol* 2012; .
11. Grossniklaus HE, Ling JX, Wallace TM, Dithmar S, Lawson DH, Cohen C, Elner VM, Elner SG, Sternberg P Jr. Macrophage and retinal pigment epithelium expression of angiogenic cytokines in choroidal neovascularization. *Mol Vis* 2002; 8:119-26. [PMID: 11979237].
12. Naug HL, Browning J, Gole GA, Gobé G. Vitreal macrophages express vascular endothelial growth factor in oxygen-induced retinopathy. *Clin Experiment Ophthalmol* 2000; 28:48-52. [PMID: 11345346].
13. Ishida S, Usui T, Yamashiro K, Kaji Y, Amano S, Ogura Y, Hida T, Oguchi Y, Ambati J, Miller JW, Gragoudas ES, Ng YS, D'Amore PA, Shima DT, Adamis AP. VEGF164-mediated inflammation is required for pathological, but not physiological, ischemia-induced retinal neovascularization. *J Exp Med* 2003; 198:483-9. [PMID: 12900522].
14. Marchetti V, Yanes O, Aguilar E, Wang M, Friedlander D, Moreno S, Storm K, Zhan M, Naccache S, Nemerow G, Siuzdak G, Friedlander M. Differential macrophage polarization promotes tissue remodeling and repair in a model of ischemic retinopathy. *Scientific Reports* 2011; 1:76-[PMID: 22355595].
15. Mo FM, Proia AD, Johnson WH, Cyr D, Lashkari K. Interferon gamma-inducible protein (IP-10) and eotaxin are associated with age-related macular degeneration. *Invest Ophthalmol Vis Sci* 2010; [PMID: 20220052].
16. Aguilar-Mahecha A, Kuzyk MA, Domanski D, Borchers CH, Basik M. The effect of pre-analytical variability on the measurement of MRM-MS-based mid- to high-abundance plasma protein biomarkers and a panel of cytokines. *PLoS ONE* 2012; 7:e38290-[PMID: 22701622].
17. Evensen L, Micklem DR, Blois A, Berge SV, Aarsæther N, Littlewood-Evans A, Wood J, Lorens JB. Mural cell associated VEGF is required for organotypic vessel formation. *PLoS ONE* 2009; 4:e5798-[PMID: 19495422].
18. Lau CH, Taylor AW. The immune privileged retina mediates an alternative activation of J774A.1 cells. *Ocul Immunol Inflamm* 2009; 17:380-9. [PMID: 20001256].
19. Denlinger LC, Fiset PL, Garis KA, Kwon G, Vazquez-Torres A, Simon AD, Nguyen B, Proctor RA, Bertics PJ, Corbett JA. Regulation of inducible nitric oxide synthase expression by macrophage purinoreceptors and calcium. *J Biol Chem* 1996; 271:337-42. [PMID: 8550583].
20. Corbett JA, Kwon G, Misko TP, Rodi CP, McDaniel ML. Tyrosine kinase involvement in IL-1 β -induced expression of iNOS by beta-cells purified from islets of Langerhans. *Am J Physiol Cell Physiol* 1994; 267:C48-54. [PMID: 7519400].
21. Kasaoka M, Ma J, Lashkari K. c-Met modulates RPE migratory response to laser-induced retinal injury. *PLoS ONE* 2012; 7:e40771-[PMID: 22808260].
22. Rowlands E, Ionides ACW, Chinn S, Mackinnon H, Davey CC. Reduced incidence of retinopathy of prematurity. *Br J Ophthalmol* 2001; 85:933-5. [PMID: 11466248].
23. Quintyn JC, Bresseur G. Subretinal fluid in primary rhegmatogenous retinal detachment: physiopathology and composition. *Surv Ophthalmol* 2004; 49:96-108. [PMID: 14711443].
24. Ricker LJAG, Kijlstra A, Kessels AGH, de Jager W, Liem ATA, Hendrikse F, La Heij EC. Interleukin and growth factor levels in subretinal fluid in rhegmatogenous retinal detachment: a case-control study. *PLoS ONE* 2011; 6:e19141-[PMID: 21556354].
25. Stone J, Chan-Ling T, Pe'er J, Itin A, Gnessin H, Keshet E. Roles of vascular endothelial growth factor and astrocyte degeneration in the genesis of retinopathy of prematurity. *Invest Ophthalmol Vis Sci* 1996; 37:290-9. [PMID: 8603833].
26. Stone J, Itin A, Alon T, Pe'er J, Gnessin H, Chan-Ling T, Keshet E. Development of retinal vasculature is mediated by

- hypoxia-induced vascular endothelial growth factor (VEGF) expression by neuroglia. *J Neurosci* 1995; 15:4738-47. [PMID: 7623107].
27. Hoeben A, Landuyt B, Highley MS, Wildiers H, Van Oosterom AT, De Bruijn EA. Vascular endothelial growth factor and angiogenesis. *Pharmacol Rev* 2004; 56:549-80. [PMID: 15602010].
 28. Chang SH, Kanasaki K, Gocheva V, Blum G, Harper J, Moses MA, Shih S-C, Nagy JA, Joyce J, Bogyo M, Kalluri R, Dvorak HF. VEGF-A induces angiogenesis by perturbing the cathepsin-cysteine protease inhibitor balance in venules, causing basement membrane degradation and mother vessel formation. *Cancer Res* 2009; 69:4537-44. [PMID: 19435903].
 29. Witmer AN, Vrensen GF, Van Noorden CJ, Schlingemann RO. Vascular endothelial growth factors and angiogenesis in eye disease. *Prog Retin Eye Res* 2003; 22:1-29. [PMID: 12597922].
 30. Nagy JA, Dvorak AM, Dvorak HF. VEGF-A and the induction of pathological angiogenesis. *Annual Review of Pathology: Mechanisms of Disease* 2007; 2:251-75. [PMID: 18039100].
 31. Boulton M, Chai Wong H, Rothery S, Marshall J. Formation of “vessel-like” structures by retinal capillary endothelial cells in culture. *Graefes Arch Clin Exp Ophthalmol* 1990; 228:377-81. [PMID: 2401423].
 32. Otani A, Takagi H, Suzuma K, Honda Y. Angiotensin II potentiates vascular endothelial growth factor–induced angiogenic activity in retinal microcapillary endothelial cells. *Circ Res* 1998; 82:619-28. [PMID: 9529167].
 33. Xiaozhuong Z, Luo XQ, Jiang JB, Huang SQ, Yan J, Che R. Isolation and characterization of fetus human retinal microvascular endothelial cells. *Ophthalmic Res* 2010; 44:125-30. [PMID: 20523104].
 34. Bakunowicz-Lazarczyk A, Sulkowski S, Moniuszko T. Comparative studies of morphological changes and interleukin concentration in subretinal fluid of patients with retinal detachment. *Ophthalmologica* 1999; 213:25-9. [PMID: 9838254].
 35. Liu Y, Yang X, Guo C, Nie P, Liu Y, Ma J. Essential role of MFG-E8 for phagocytic properties of microglial cells. *PLoS ONE* 2013; 8:e55754-[PMID: 23405209].
 36. Lee BJ, Kim JH, Heo H, Yu YS. Delayed onset atypical vitreo-retinal traction band formation after an intravitreal injection of bevacizumab in stage 3 retinopathy of prematurity. *Eye (Lond)* 2012; 26:903-09. [PMID: 22699977].

Articles are provided courtesy of Emory University and the Zhongshan Ophthalmic Center, Sun Yat-sen University, P.R. China. The print version of this article was created on 21 June 2014. This reflects all typographical corrections and errata to the article through that date. Details of any changes may be found in the online version of the article.